Modeling Effects of Strain-Modulated Membrane Capacitance and Conductance of K^+ Inward Rectifier on Conduction Velocity in Cardiac Tissue

TG McNary[1,2], FB Sachse[1,2]

[1]Bioengineering Department, University of Utah Salt Lake City, UT, USA
[2]Nora Eccles Harrison Cardiovascular Research and Training Institute, University of Utah Salt Lake City, UT, USA

Abstract

Mechanical deformation of cardiac myocytes has been shown to alter the conductance of various ion channels and possibly membrane capacitance. Here, we studied the strain-modulation of electrical membrane properties at rest. In particular we studied the conductance of the inward rectifying K^+ channel (G_{K1}) and the membrane capacitance (C_m) with respect to cellular electrophysiology and conduction velocity. For this purpose, we applied mathematical models of cardiac myocytes in computational simulations. To explore strain modulation we varied the C_m and G_{K1} in the range of $\pm$25% of their original values. Conduction velocity (Θ) decreased to 39.7 and 45.7cm/s with +25% in C_m and G_{K1} respectively. A decrease of 25% in C_m and G_{K1} caused a respective increased of 57.9 and 48.4 cm/s where 47.0 cm/s was the Θ using default values. Our study indicates that establishing the relationship between strain and G_{K1} as well as strain and C_m at myocyte level will be necessary to understand measured strain-Θ relationships in myocardium.

1. Introduction

Mechano-electric feedback (MEF) is well established as a modulator of electrophysiology of cardiac myocytes and tissue. Acute strain has been shown to alter conduction velocity (Θ) and can cause conduction block [1–5]. Strain also decreased action potential duration at 20% repolarization (APD_{20}) and increased APD at 90% repolarization (APD_{90}) of myocytes and has been suggested to prime cardiac tissue for re-entry of electrical activation [6–8]. A proper characterization of the extent of MEF will allow an understanding of electrical activity during physiologic contractions and aid in deciphering pathophysiologic states.

It is generally accepted that Θ is affected by membrane excitability, intercellular coupling, and passive membrane properties. Early models of conduction are based on these properties. However, most modeling approaches were based on the assumption that these properties are independent of strain. Experiments within the last two decades have shown that cardiac myocytes possess ion channels that exhibit a strain-modulated conductance [9–12]. A number of experiments demonstrated depolarized resting membrane voltages when axial strain was applied to the myocytes. This was suggested to be caused by activation of non-selective stretch activated channels (SAC_{NS}) and/or by decrease in the conductance of the inward rectifying K^+ channels [10, 12, 13]. In studies on isolated murine myocytes, the conductance of the inward rectifying K^+ channel (G_{K1}) decreased by as much as 33% in response to axial strain [12].

Experimental studies of rabbit ventricular tissue showed a decrease in Θ during volume load with and without using Gd^{3+} to block SAC_{NS} [14]. This suggests the lack of SAC_{NS} involvement. Similar studies in papillary muscle using streptomycin to block SAC_{NS} led to the same conclusion [5].

Electron micrographs of strained myocytes showed a reduction in 'slack' membrane and integration of caveolae into the membrane surface [15]. These effects suggest an increase in membrane capacitance (C_m). In a study of rabbit ventricle, space constants were measured for different mechanical loads on tissue [14]. C_m values were estimated based on changes of the space constant using a bidomain model of electrical conduction [16]. This analysis suggests that C_m increases as mechanical load increases.

Strain modulation of inward rectifying K^+ channels is well established [17]. However, the effects of variation of G_{K1} in combination with variations in C_m are less understood.

The objective of this paper is to study the strain-modulation of electrical properties of cell membranes at rest, in particular G_{K1} and the membrane capacitance (C_m), with respect to cellular electrophysiology and con-

Table 1. Model parameters, symbols and values

Model parameters	Variable	Value	Units
Cellular diameter	a	8	μm
Cellular length	l	100	μm
Coupling resistance	R_c	1.25	MΩ
Membrane capacitance	C_m	95	pF
I_{K1} conductance	G_{K1}	0.50	μS

duction velocity. We used mathematical models of cardiac myocytes in computational simulations for this study.

2. Methods

This study explores potential effects of strain-modulated G_{K1} and C_m on cellular and tissue electrophysiology, in particular, Θ, upstroke velocity of the transmembrane voltage (dV_m/dt), and action potential duration (APD). Electrical conduction was described by a computational monodomain model of a one dimensional tissue strand using the cable equation as follows:

$$\frac{a}{2}\frac{\partial}{\partial x}\left(\frac{1}{\rho(x)}\frac{\partial V_m(x,t)}{\partial x}\right) = I_{ion} + C_m\frac{\partial V_m(x,t)}{\partial t} \quad (1)$$

with the cellular diameter a, the resistivity ρ, the transmembrane voltage V_m, and membrane currents I_{ion}. Resistivity ρ was calculated using the coupling resistance (R_c). The strand had a length of 2.4 mm and was discretized every 0.1 mm. Parameters of the model are presented in table 1. Myocytes were represented by the Noble et al. model of the electrophysiology of guinea-pig ventricular cells [18]. The ordinary differenctial equations underlying the arrangements were solved using the Euler method with a time step of 1μs. Intercellular currents were updated every 1 μs. A stimulus frequency of 0.5 Hz was used. The stimulus current applied to myocyte 0 was 25 nA until a threshold voltage, -50 mV, was reached. The resulting stimulus duration was kept shorter than 1 ms to avoid significant overlap of sodium and stimulus current. Simulation results were analyzed after the 10^{th} simulation.

The equations used to describe I_{K1} were as follows:

$$I_{K1} = G_{K1}\frac{[K]_e}{[K]_e + k_{m,k1}}\left(\frac{V_m - E_K}{1 + e^{\frac{(V_m - E_K - 10)1.25F}{RT}}}\right) \quad (2)$$

$$E_K = \frac{RT}{F} ln\left(\frac{[K^+]_e}{[K^+]_i}\right) \quad (3)$$

with the respective extra- and intracellular K^+ concentrations $[K]_e$ and $[K]_i$, the Michaelis constant $k_{m,k1}$, the Nernst potential for K^+ (eq 3) E_K, the Faraday's constant F , the gas constant R , and the absolute temperature T.

To explore strain modulation we varied both the original C_m and the original G_{K1} (table 1) in the range of $\pm$25% in 5% increments. The analysis yielded Θ, dV_m/dt, APD, and resting membrane voltage.

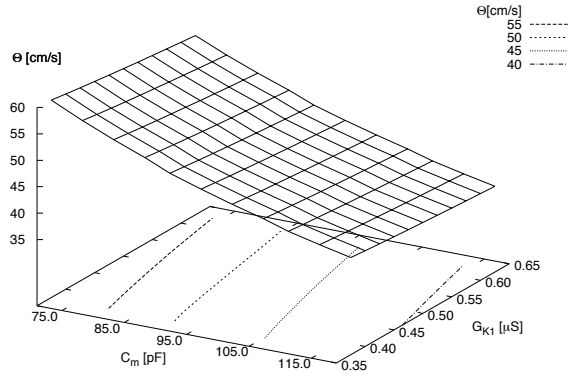

Figure 1. Simulated Θ with C_m and G_{K1}. The negative relationship between Θ is larger for C_m than G_{K1}. The effect is near linear for both variables.

3. Results

We performed simulations varying C_m and G_{K1} using the described model of electrical conduction in tissue. As C_m was incrementally increased from -25 to +25% there was a consistent decrease in Θ, dV_m/dt, and an increase in APD_{90}. A similar increase in G_{K1} caused a decrease in Θ, dV_m/dt, and in APD_{90}. All changes to the resting membrane voltage, originally at 92.1 mV, through varied values of C_m and G_{K1} were $<$2%.

Increases in C_m caused a near linear decrease in Θ (Fig 1). When C_m was increased from 71.25 (holding G_{K1} constant at 0.50 μS) to 76.0 pF the Θ decreased by 4.6% cm/s from 57.94 to 55.3 cm/s. As C_m increased the change in Θ decreased such that the difference in Θ between the largest two iterations of capacitance in the simulation had a decrease of 3.1% cm/s. Over all, Θ increased by 23.4% and decreased by 18.3% with a respective 25% decrease and increase in C_m.

A decreasing relationship was also found as G_{K1} was increased . The trend for the change in Θ to decrease as G_{K1} increased also held, though smaller in magnitude. The decrease in Θ from changing G_{K1} from 0.375 to 0.400 μS (holding C_m constant at 95 pF) was 0.32 cm/s from 48.40 to 48.08 cm/s, while the increase from 0.600 to 0.625 μS was 0.22 cm/s. Θ increased by 3.1% and decreased by 2.6% with a respective 25% decrease and increase in G_{K1}.

When C_m was increased from -25 to -20% the decrease in dV_m/dt was 3.0%. An increase from +20 to +25%the caused a decrease in dV_m/dt of 2.2%. When C_m was in-

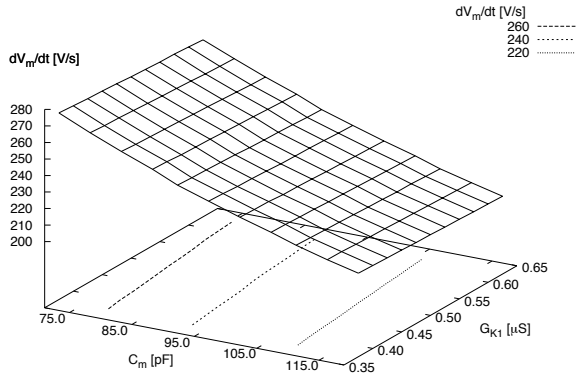

Figure 2. Simulated dV_m/dt for varied C_m and G_{K1}. As with Θ, the negative relationship between C_m and dV_m/dt was larger than that with G_{K1}. The change in response to C_m appeared to be near linear.

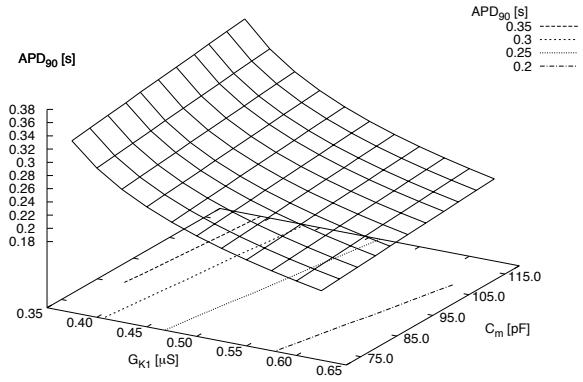

Figure 3. Change in APD_{90} with respect to varied C_m and G_{K1}. APD is effected more dramatically by a change in G_{K1}, than by a change in capacitance. Note that the x-axis is G_{K1} and the y-axis is C_m.

creased from -25% to 0% dV_m/dt decreased by 13.1% from 269.7 V/s. The increase in C_m from 0% to +25% caused dV_m/dt to decreasing by 10.9% from 234.4 V/s (Fig 2).

The effects of G_{K1} were smaller on dV_m/dt compared to the effects of C_m. Increasing the conductance from -25% to 0% decreased upstroke velocity by only 1%, while the change from 0% to +25% G_{K1} decreased dV_m/dt by less than 1%.

The change in APD_{90} remained almost constant at 1% change for every 5% increment change in C_m. APD_{90} decreased by 4.9% and increased by 4.6% with a coinciding decrease and increase of 25% C_m.

The change in APD_{90} was closer to exponential while G_{K1} was varied (Fig 3). When G_{K1} was increased from -25 to -20% APD_{90} decreased from 357.2 ms by 10.1%, but the total change from -25% to normal conductance was 31.7%. The change from normal conductance to +25% was 20%. The maximal variation caused an APD_{90} of 195.1 ms, 4.0% smaller than at +20% conductance.

4. Discussion and conclusions

It has been hypothesized that increased strain will induce an increase in C_m [14, 15]. As suggested by the presented simulations, a small increase in C_m will cause a large reduction in Θ. However, the extent of C_m changes during physiological function is still unknown as well as the relationship between strain and C_m.

The effects of varied G_{K1} in the same range as C_m variations are less significant in the presented simulations with regards to dV_m/dt and Θ. For example, it would take more than a 25% decrease in G_{K1} to match the effects of a 5% decrease in C_m for both dV_m/dt and Θ.

As C_m was the dominant determinant of dV_m/dt and Θ, G_{K1} was the dominant determinant of APD_{90}. For a 5% decrease in G_{K1}, there would need to be an increase greater than 25% in C_m for the same effect. This implies that conductances of depolarizing ion channels will in general have a larger effect on APD_{90} than C_m.

A graphical representation of the effects of G_{K1} and C_m on APD_{90}, Θ, and dV_m/dt is shown in Fig. 4. As strain increases G_{K1} decreases while it is hypothesized that C_m will increase [12–15]. Such an effect would imply a decrease in Θ and an increase in APD_{90}. We suggest that these results are highly relevant for dissection of the various biophysical mechanisms that underlie measured strain-Θ relationships.

Limitations of this study. Limitations are associated with the rather simple model of cellular and tissue electrophysiology used in this study. We did not intent to develop a physiologically accurate model, but focussed on two important aspects of MEF. We characterized the effects of varied G_{K1} and C_m that may occur due to stretch. There are a number of other stretch activated ion channels that were not taken into account in our simulations. A more complete description of stretch effects has been recently published [12]. Here, three groups of stretch-sensitive ion channels were distinguished. One group was a conglomeration of outwardly rectifying K^+ channels (I_{oth}). The other groups were the SAC_{NS} and channels responsible for I_{K1}. Using this approach, a modeling study showed that the combination of I_{oth} and I_{ns} will decrease the APD_{20} while increasing APD_{90} [19]. Considering the

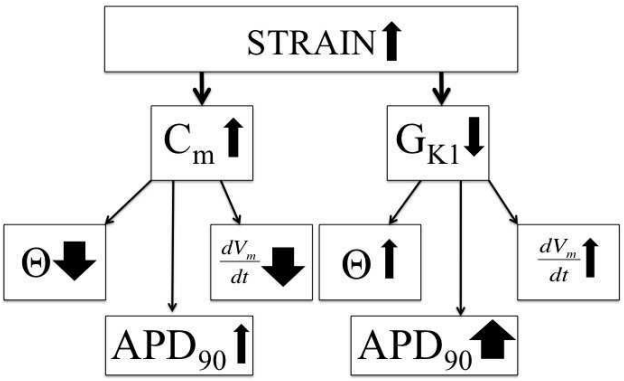

Figure 4. Summary of the effects of C_m and G_{K1} on APD_{90}, Θ, and dV_m/dt. The thickness of the arrows represent the magnitude of change.

small effects of varied C_m on APD_{90}, it is conceivable that stretch induced changes on C_m will remain too small to prevent shortening of APD_{20} or lengthening of APD_{90} while causing a decrease in Θ.

Acknowledgements

This work was funded by the Richard A. Harrison and Nora Eccles Fund for Cardiovascular Research and awards from the Nora Eccles Treadwell Foundation.

References

[1] Zabel M, Portnoy S, Franz MR. Effect of sustained load on dispersion of ventricluar repolarization and conduction time in the isolated intact rabbit heart. J Cardiovasc Electrophysiol January 1996;7:9–16.

[2] Reiter MJ, Landers M, Zetelaki Z, Kirchhof CJH, Allessie MA. Electrophysiological effects of accute dilation in the isolated rabbit heart. Circulation 1997;96:4050–4056.

[3] Sung D, Mills RW, Schettler J, Narayan SM, Omens JH, McCulloch AD. Ventricular filling slows epicardial conduction and increases action potential duration in an optical mapping study of the isolated rabbit heart. J Cardiovasc Electrophysiol Jul 2003;14(7):739–49.

[4] Eijsbouts SCM, Majidi M, van Zandvoort M, Allessie MA. Effects of acute atrial dilation on heterogeneity in conduction in the isolated rabbit heart. J Cardiovasc Electrophysiol Mar. 2003;14:269–278.

[5] McNary TG, Sohn K, Taccardi B, Sachse FB. Experimental and computational studies of strain-conduction velocity relationships in cardiac tissue. Prog Biophys Mol Biol 2008; 97:383–400.

[6] Zabel M, Franz MR. Mechanical triggers and facilitators of cardiac excitation and arrhythmias. In Kohl P, Sachs F, Franz MR (eds.), Cardiac Mechano-Electric Feedback and Arrhythmias. Elsevier Saunders, 2005; 119–26.

[7] Taggart P, Sutton P. Load dependence of ventricular repolarization. In Koh P, Sachs F, Franz MR (eds.), Cardiac Mechano-Electric Feedback and Arrhythmias. Elsevier Saunders, 2005; 191–197.

[8] Taggart P, Sutton P. Termination of arrhythmias by hemodynamic unloading. In Kohl P, Sachs F, Franz MR (eds.), Cardiac Mechano-Electric Feedback and Arrhythmias. Elsevier Saunders, 2005; 315–320.

[9] Ruknudin A, Sachs F, Bustamante JO. Stretch-activated ion channels in tissue-cultured chick heart. Am J Physiol Heart Circ Physiol 1993;264(33):H960–972.

[10] Zeng T, Bett GCL, Sachs F. Stretch-activated whole cell currents in adult rat cardiac myocytes. Am J Physiol 2000; 278:H548–H557.

[11] Belus A, White E. Streptomycin and intracellular calcium modulate the response of single guinea-pig ventricular myocytes to axial stretch. J Physiol Jan 2003;15(546):501–9.

[12] Dyachenko V, Husse B, Rueckschloss U, Isenberg G. Mechanical deformation of ventricular myocytes modulates both trpc6 and kir2.3 channels. Cell Calcium 2008;.

[13] Isenberg G, Kazanski V, Kondratev D, Gallitelli MF, Kiseleva I, Kamkin A. Differential effects of stretch and compression on membrane currents and $[na^+]_c$ in ventricular myocytes. Prog Biophys Mol Biol 2003;82:43–56.

[14] Mills RW, Narayan SM, McCulloch AD. Mechanisms of conduction slowing during myocardial stretch by ventricular volume loading in the rabbit. Am J Physiol Circ Physiol 2008;295:H1270–H1278.

[15] Kohl P, Cooper PJ, Holloway H. Effects of acute ventricular volume manipulation on in situ cardiomyocyte cell membrane configuration. Prog Biophys Mol Biol 2003;82(1-3):222–227.

[16] Henriquez CS. Simulating the electrical behaviour of cardiac tissue using the bidomain model. Crit Rev Biomed Engin 1993;21(1):1–77.

[17] Patel AJ, Honoré E. Potassium-selective cardiac mechanosensitive ion channels. In Kohl P, Sachs F, Franz MR (eds.), Cardiac Mechano-Electric Feedback and Arrhythmias. Elsevier Saunders, 2005; 11–20.

[18] Noble D, Varghese A, Kohl P, Noble P. Improved guinea-pig ventricular cell model incorporating a diadic space, I_{Kr} and I_{Ks}, and length- and tension-dependend processes. Can J Cardiol Jan. 1998;14(1):123–134.

[19] Healy SN, McCulloch AD. An ionic model of stretch-activated and stretch-modulated currents in rabbit ventricular myocytes. Europace 2005;7(S128-S134).

Address for correspondence:

Name: Thomas McNary
Full postal address: Nora Eccles Harrison Cardiovascular Research and Training Institute,University of Utah
95 S. 2000 E. Salt Lake City, UT 84112
E-mail address: mcnary@cvrti.utah.edu